JOURNAL OF THE STRUCTURAL DIVISION

CREEP AND SHRINKAGE IN REACTOR CONTAINMENT SHELLS

By Zdeněk P. Bažant,[1] M. ASCE, Domingo J. Carreira,[2] and Adolf Walser[3]

INTRODUCTION

In the design of a concrete containment shell for a nuclear reactor, the limit state is of primary importance and stresses due to service loads are of secondary importance because cracking of concrete is admissible; the leak-tightness of the containment is assured by the steel liner. Nevertheless, to achieve high durability and good composite action, and to properly choose the percentage, diameter, and spacing of mild reinforcement, it is desirable to limit the width and spacing of cracks and the strains in the liner under service loads. For this reason, evaluation of stresses due to service loads is also required in the design, even though it is clearly of secondary concern. One of the service loads is the effect of creep and shrinkage. According to the current design practice (15), attention is paid only to the effects of the overall creep and shrinkage of concrete walls upon the strain of the liner and the prestress loss. Consideration of the differences in creep and shrinkage between various structural parts and across the walls of the shell is not specifically required (15,17).

The purpose of this study, which is based on Ref. 3, is to show that, although the effects of differences in creep and shrinkage do not represent a primary consideration in design, they are not smaller than the effects of differences in thermal expansion due to sustained operating temperature gradient, which, though being of similar character, are being considered in design (15,18). It follows that in a fully consistent approach to design, the differences in creep and shrinkage and the differences in thermal expansion due to sustained operating temperature should either be both considered in design or both disregarded. This conclusion, of course, only points out a way of theoretical improvement of the design process and certainly does not imply that the present method

Note.—Discussion open until March 1, 1976. To extend the closing date one month, a written request must be filed with the Editor of Technical Publications, ASCE. This paper is part of the copyrighted Journal of the Structural Division, Proceedings of the American Society of Civil Engineers, Vol. 101, No. ST10, October, 1975. Manuscript was submitted for review for possible publication on January 25, 1975.

[1]Staff Consultant, Sargent & Lundy, Chicago, Ill. and Prof. of Civ. Engrg., Northwestern Univ., Evanston, Ill.

[2]Sr. Struct. Engrg. Specialist, Sargent & Lundy, Chicago, Ill.

[3]Chf. Struct. Engrg. Specialist, Sargent & Lundy, Chicago, Ill.

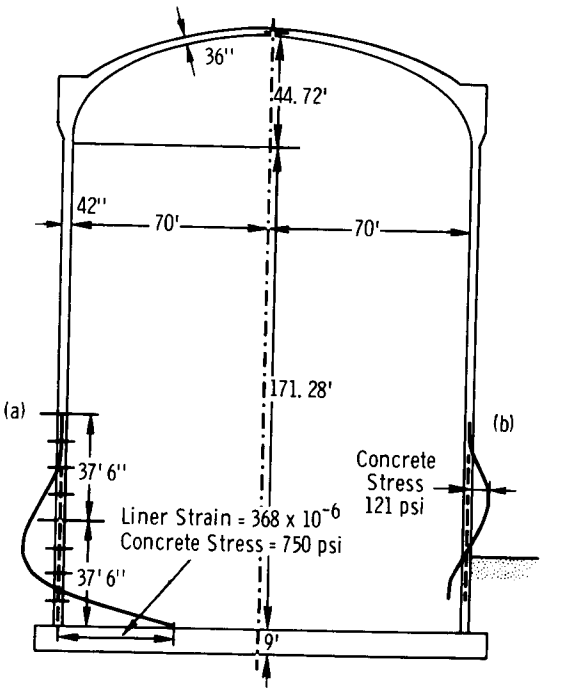

FIG. 1.—Vertical Section of Typical Containment Shell and Effects of Shrinkage Difference between Shell and Foundation Slab (1 ft = 0.305 m; 1 in. = 25.4 mm; 1 psi = 6.89 kN/m²)

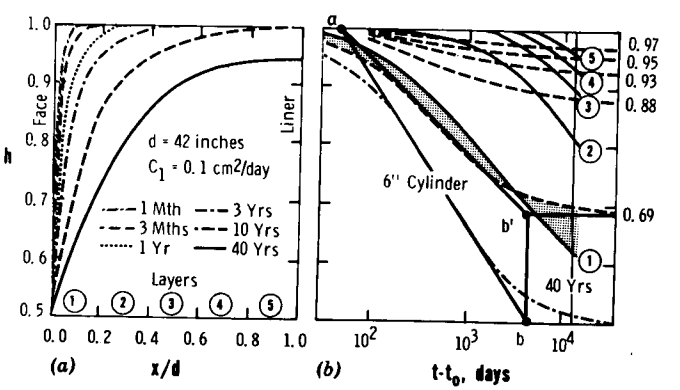

FIG. 2.—Drying of Concrete Wall and its Comparison with Drying of Standard Cylinder

of analysis is inadequate, because the effects of sustained operating temperature are rather small themselves.

In addition, this study has the purpose of demonstrating how the age-adjusted effect modulus method (2,6) [a recently-introduced method that is superior in accuracy as well as simplicity to other known approximate linear methods for the prediction of creep effects (6,9)] can be applied to reactor containment shells. Also, a new simple approximate method of determining the effect of the drying rate of an element within the concrete mass upon its unrestrained creep and shrinkage will be proposed.

A typical reactor containment shell (Fig. 1) will be considered in numerical calculations and, for the sake of simplicity, it will be assumed that the prestress is sufficient to prevent cracking. Actually, according to the stress values found, cracking will occur and will substantially relieve the values found herein. Therefore, the numerical values presented must be regarded strictly as comparative values, i.e., values that may be compared with the effect of operating temperature which is normally also evaluated under the assumption of no cracking. The actual values with cracking will undoubtedly be much smaller but their calculation is beyond the scope of this paper and necessitates a complex finite element program whose development has not yet been completed.

Simple Method of Predicting Drying-Induced Differences in Creep and Shrinkage across Wall

On the inside face of the containment wall, evaporation of water is prevented by a steel liner, while the outside face is exposed to the climate whose annual average relative humidity will be considered as $h_e = 50\%$. This gives a somewhat more severe drying than the usual climate in the northern and northeastern United States. Comparing the limited shrinkage data for the concrete of the containment considered with the much more extensive data of Hansen and Mattock (12), it was concluded that the drying diffusivity of both concretes was about the same. Thus, according to the data fits in Ref. 7, the diffusivity of a nearly saturated concrete is considered to be $C_1 = 0.25$ cm^2/day at the age of 7 days and $C_1 = 0.10$ cm^2/day as the long-time average (in a massive wall). These values decrease about 20 times (5) as the pore humidity of concrete drops from 90%-65%. Taking these facts into account, the distribution of pore humidity across the wall of thickness $d = 42$ in. (1,067 mm) at various times from the start of drying (assumed to occur at age $t_o = 10$ days) can be predicted from the charts given in Ref. 5 Fig. 2(a), in which $x = 0$ is the drying face, shows the distribution. These predictions are approximately based on the average of the operating temperatures across the wall, and this average is very near the room temperature.

For calculations, the wall will now be divided into five layers [Fig. 2(a)]. (With regard to the steep variation of pore humidity and shrinkage stress shown in Figs. 2 and 3, a subdivision in only five layers cannot yield high accuracy. However, in view of the well-known inaccuracies of shrinkage, creep, and drying laws, as well as the large statistical scatter of these phenomena, especially in field conditions, the subdivision error is unimportant.) Determining the average values of the pore humidity, h, within each layer at various times, one can construct the drying curves of the individual layers [Fig. 2(b)]. It is necessary

to predict from these curves the unrestrained drying creep and shrinkage of the individual layers. Curiously, no attention seems to have been paid to this practical problem so far; therefore, the following approximate method is proposed.

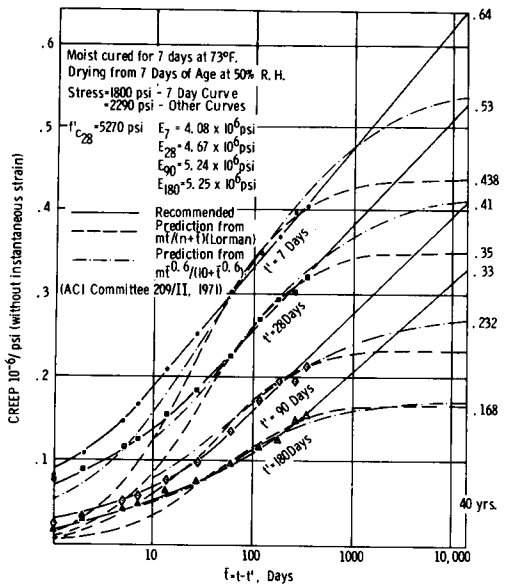

FIG. 3.—Extrapolation of Creep Test Data for Containment Concrete (1 psi = 6.89 kN/m²)

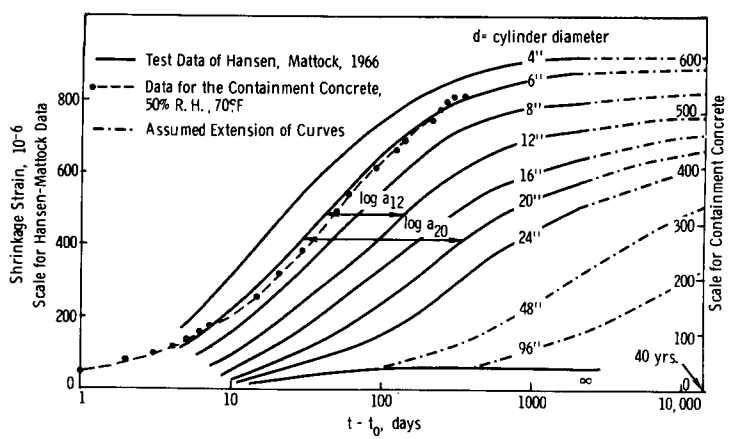

FIG. 4.—Extrapolation of Shrinkage Data for Containment Using Test Data of Hansen and Mattock (12)

The objective is to find the environmental relative humidities, h_e, that will cause in standard 6-in. (152-mm) cylinders about the same acceleration of creep as the drying curves of the individual layers. The curves of the average humidity

of 6-in. (152-mm) cylinders at various h_e levels will be approximately assumed to be proportional to the curve at $h_e = 50\%$, which has been predicted for the concrete at hand from the graphs in Ref. 5, and is shown with a dashed curve in Fig. 2(*b*). In comparing various drying curves, it is important to realize that the acceleration of creep due to simultaneous drying is not caused by a lower water content but by the mobility of water during drying. After drying ends, the creep is, in fact, less than that in a saturated concrete. Thus, it is necessary to assess the drying rates from Fig. 2(*b*). To this end, note that in a log-scale a change in the drying rate corresponds to a horizontal shift of the whole curve [because $\log (at) = \log t + \log a$]. Therefore, it seems reasonable to assume that any drying curve that encloses roughly equal areas (in log-scale) on the left and right of the given curve yields about the same acceleration of creep. Accordingly, the drying curve of a 6-in. (152-mm) cylinder at $h_e = 50\%$ may be scaled vertically in a constant ratio so as to satisfy this condition as indicated by the dashed curves in Fig. 2(*b*).

As a result, it can be expected that layers 1-5 will creep similarly as 6-in. (152-mm) cylinders that dry at environmental humidities [Fig. 2(*b*)]:

$$h_e = 0.69, 0.88, 0.93, 0.95, 0.97 \quad \ldots\ldots\ldots\ldots\ldots\ldots\ldots\ldots\ldots\ldots (1)$$

Only the effects of creep and shrinkage at $t = 40$ yr of age on a wall loaded from age $t_o = 90$ days will be considered herein. For these values of t and t_o, the creep coefficient, $\phi(t, t_o)$ of a 6-in. (152-mm) cylinder drying at 50% humidity has been determined by extrapolation of the short-time creep data to be 2.15 (Fig. 3). According to the test data of L'Hermite, et al. (13) and others, the creep of test specimens at 100% humidity is about 0.5 of that at 50% humidity and a linear interpolation approximately holds for the intermediate humidities. Thus, the creep coefficient for humidities $h_e \geq 0.5$ is approximately $\phi(t, t_o) = \phi_{50}(t, t_o)(1.5 - h_e)$, in which the subscript, 50, refers to 50% humidity. Substituting the previous values of h_e yields creep coefficients of layers $i = 1, \ldots 5$:

$$\phi_i = 1.74, 1.33, 1.23, 1.18, 1.14, \quad \text{for} \quad t = 40 \text{ yr} \quad \text{and} \quad t_o = 90 \text{ days} \quad \ldots . (2)$$

Furthermore, these values should be corrected for the effect of temperature and, in an accurate analysis, both the temperature gradient when the reactor operates and the gradient before the operation starts should be taken into account. However, for the sake of simplicity, the effect of the temperature gradient upon creep will not be considered in the present analysis. This simplification is certainly not too serious as far as the average of the temperatures across the wall is concerned, because this average is only slightly below it before the operation.

For predicting creep effects by the age-adjusted effective modulus method, one must determine the aging coefficients, χ, from Table 1 in Ref. 2 (from which the lower left quarter applies herein). For layers 1-5, this gives

$$\chi_i = 0.89, 0.88, 0.87, 0.87, 0.87 \quad \ldots\ldots\ldots\ldots\ldots\ldots\ldots\ldots\ldots\ldots (3)$$

Finally, one needs the age-adjusted effective modulus (2), which is computed as

$$E''(t, t_o) = \frac{E(t_o)}{1 + \chi(t, t_o)\,\phi(t, t_o)} \quad \ldots\ldots\ldots\ldots\ldots\ldots\ldots\ldots\ldots\ldots (4)$$

in which $E(t_o)$ = Young's modulus at $t_o = 90$ days, which has been determined by tests as 5.24×10^6 psi. Thus, for layers 1-5 (1 psi = 6.89 kN/m^2):

$$E_i'' = 2.06 \times 10^6 \text{ psi}, 2.41 \times 10^6 \text{ psi}, 2.54 \times 10^6 \text{ psi}, 2.59 \times 10^6 \text{ psi}, 2.63$$

$$\times 10^6 \text{ psi} \quad \text{for} \quad t = 40 \text{ yr} \quad \text{and} \quad t_o = 90 \text{ days} \quad \ldots\ldots\ldots\ldots\ldots\ldots (5)$$

For the differences in shrinkage, one may consider the fact that, in contrast with the acceleration of creep by drying, the shrinkage strain is determined essentially be the pore humidity level (or magnitude of water loss), rather than by the drying rate. Thus, for $t = 40$ yr, shrinkage would best be determined on the basis of the final h-values of the five curves, which are slightly less than the values in Eq. 1. Then, however, h_e would have to be considered to be different in each layer. Also, maximum shrinkage stresses usually occur before the end of service life (2), and then the differences between h_e and the actual end values of h for the layers in Fig. 2(*b*) are less than those for $t = 40$ yr.

Consequently, it will be assumed again, for the sake of simplicity, that each of the five layers, if unrestrained, would shrink the same as the 6-in. (152-mm) cylinder at humidity h_e, obtained previously (Eq. 1). This corresponds to the assumption that the differences in unrestrained shrinkage are determined by the time-averages of the pore humidities in layers 1-5.

If the shrinkage tests (of 1 yr duration) that have been carried out for the containment shell under consideration are extrapolated with the aid of Hansen and Mattock's data (12), the shrinkage of a 6-in. (152-mm) cylinder at humidity $h_e = 0.5$ at the age of 40 yr is found to be 600×10^{-6} (Fig. 4). To determine shrinkage strain ϵ_{sh} at other humidities h_e, one may consider that ϵ_{sh} is approximately proportional to $1\text{-}0.95\, h_e^3$, as can be confirmed, e.g., by comparison with the data of L'Hermite, et al. (13). Using this function and the values of h_e in Eq. 1, the unrestrained 40-yr shrinkage strain of layers $i = 1, \ldots 5$ is estimated as (1 psi = 6.89 kn/m^2):

$$\epsilon_{sh} = 487 \times 10^6, 312 \times 10^6, 198 \times 10^6, 144 \times 10^6, 126 \times 10^6,$$

$$\text{for} \quad t = 40 \text{ yr} \quad \text{and} \quad t_o = 10 \text{ days} \quad \ldots\ldots\ldots\ldots\ldots\ldots\ldots\ldots (6)$$

To determine creep coefficients, the creep data of limited duration (1 yr) must be first extrapolated to a 40-yr duration of creep. The question of the proper extrapolation method is particularly important when such a long duration as this is considered. In the past, the use of a hyperbolic expression has been widespread, but from recent long-time creep tests it became apparent that this expression seriously underestimates creep when extrapolation to more than 2 yr is attempted. Properly, the creep data must be extrapolated by straight or upward curving lines in log-time scale. Using this method, the creep coefficient, ϕ, of a 6-in. (152-mm) cylinder drying at 50% humidity has been determined to be 2.52 for $t = 40$ yr and $t_o = 10$ days, the assumed start of drying. Scaling this value down in the same ratios as before, one obtains for layers $i = 1, \ldots 5$:

$$\phi_i = 2.11, 1.61, 1.48, 1.43, 1.38 \quad \text{for} \quad t = 40 \text{ years} \quad \text{and} \quad t_o = 10 \text{ days} \quad \ldots (7)$$

From Table 1 in Ref. 2, one may determine $\chi(t_1, t_o)$ similarly as before:

$$\chi_i = 0.68, 0.65, 0.63, 0.61, 0.60 \quad \ldots\ldots\ldots\ldots\ldots\ldots\ldots\ldots\ldots\ldots (8)$$

Elastic modulus E at $t_o = 10$ days was found to be 4.08×10^6 psi (28.1×10^6 kN/m^2). Thus (1 psi = 6.89 kN/m^2):

$E_i'' = 2.44 \times 10^6$ psi, 2.05×10^6 psi, 1.93×10^6 psi, 1.87×10^6 psi, 1.83×10^6 psi, for $t = 40$ yr and $t_o = 10$ days . . . . . (9)

Stress Redistribution within Cross Section of Wall

Among all methods presently known, the age-adjusted effective modulus method (2,6) has been shown (6) to be superior in accuracy to other known methods (with regard to the exact solution according to the principle of superposition); this has been recently confirmed by numerous practical examples and systematic numerical comparisons by Bruegger (9). This method has the advantage of not requiring solution of any differential equation, since the problem is reduced to the analysis of an elastic structure according to the quasi-elastic stress-strain law whose uniaxial form is

$$\Delta\epsilon(t) = \frac{\Delta\sigma(t)}{E''(t, t_o)} + \frac{\sigma(t_0)}{E(t_o)}\phi(t, t_o) + \Delta\epsilon_{sh} \quad \ldots\ldots\ldots\ldots\ldots\ldots (10)$$

in which ϵ, σ = strain and stress; and Δ refers to changes from time t_o (the start of straining of the structure). This relation is exact when $\Delta\epsilon(t)$ is proportional to $\phi(t, t_o)$ at any time t, which appears to be a good assumption in most cases (6). The age-adjusted effective modulus (2), $E''(t, t_0)$, introduces the effect of creep due to the gradual stress changes, $d\sigma$, which are induced in the structure. It also takes into account the fact that both the creep coefficient and the elastic modulus for the stress changes after time t_o are less, the higher the age (aging effect).

Shrinkage Effect.—In analogy with Eq. 10 for $\sigma(t_0) = 0$, the biaxial strain change, $\Delta\epsilon$, and the biaxial stress changes, $\Delta\sigma_i$, in layers $i = 1, \ldots 5$ from time t_o to time t satisfy the equations:

$$\Delta\epsilon = \Delta\sigma_i \frac{1-\nu}{E_i''} + \Delta\epsilon_{shi} \quad (i = 1, \ldots 5) \quad \ldots\ldots\ldots\ldots\ldots\ldots (11)$$

in which the condtions of equal strain across the wall, and of equal biaxial stresses $\sigma_{yi} = \sigma_{zi} = \sigma_i$ in the plane of the wall, are implied. Also implied is the assumption that there is no change in the curvature of wall. The conditions of equilibrium are

$$\sum_{i=1}^{5} A_i \Delta\sigma_i + \left(\frac{E_l A_l}{1-\nu_l} + E_p A_p + E_s A_s\right)\Delta\epsilon = 0 \quad \ldots\ldots\ldots\ldots\ldots\ldots (12)$$

in which E_l, E_p, and E_s = Young's moduli of steel liner, prestressing tendons, and nonprestressed reinforcement; ν_l = Poisson's ratio of liner ≈ 0.33; and ν = Poisson's ratio of concrete ≈ 0.18. (Poisson's ratio for creep of concrete under severe drying conditions is much less than 0.18, but such conditions exist only in a shallow surface layer.) Furthermore, A_i, A_l, A_p, A_s, = cross-sectional areas of the layer of wall, of the liner, of the prestressing tendons, and of the nonprestressed reinforcement (per unit length of wall).

The values, $A_i = d/5$, $A_l = 0.25$ sq in./in. (0.635 cm^2/cm), $A_p = 0.210$ sq in./in. (0.533 cm^2/cm) and $A_s = 0.126$ sq in./in. (0.320 cm^2/cm), were considered. The radius of the cylindrical curvature of the wall is assumed to be much larger than its thickness $d = 42$ in. (1,067 mm). Eq. 12 implies equal strain in concrete and in prestressing tendons. In reality, this is not assured because the tendons are unbonded. However, because cross sections along the shell are in a similar stress state, the effect of equalization of tendon strain along the height will be small, and so Eq. 12 is acceptable.

Using the values from Eqs. 9 and 6, the solution of Eqs. 11 and 12 gives the following changes due to shrinkage from $t_o = 10$ days to $t = 40$ yr in the middle of layers 1-5 (1 psi = 6.89 kN/m^2):

$\Delta\sigma_i = 582$ psi, 265 psi, -12 psi, -153 psi, -207 psi; $\Delta\epsilon = -202 \times 10^{-6}$ (13)

Similar computations have been carried out for $t = 1$ month, 3 months, 1 yr, 3 yr, and 10 yr. The results are plotted in Fig. 5. (The surface values

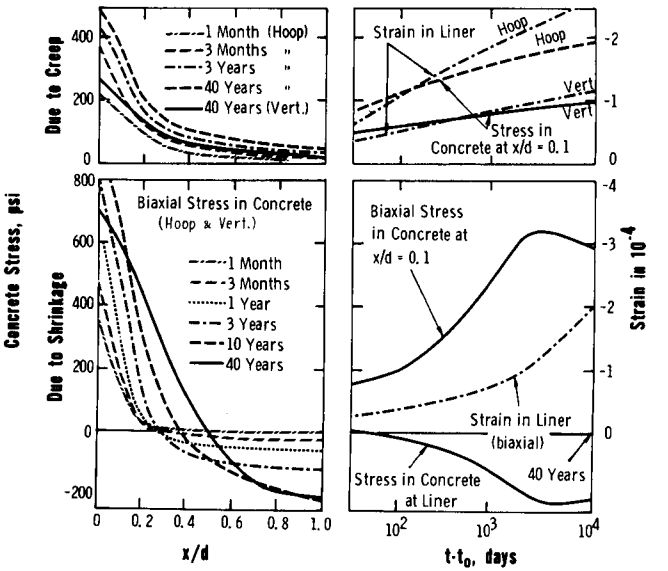

FIG. 5.—Approximate Concrete Stress and Liner Strains Caused by Shrinkage and Creep in General Cross Section of Wall (No Cracking Assumed)

shown were obtained by graphical extrapolation, plotting smooth curves through the values at midpoints of layers.)

Creep Due to Prestress.—In analogy with Hooke's law, the stress-strain relations of the age-adjusted effective modulus method (2) read

$$\Delta\sigma_{zi} = (\Delta\epsilon_z + \nu\Delta\epsilon_y - \Delta\epsilon_z'' - \nu\Delta\epsilon_y'')\frac{E_i''}{1-\nu^2} \quad \ldots\ldots\ldots\ldots\ldots\ldots (14a)$$

$$\Delta\sigma_{yi} = (\nu\Delta\epsilon_z + \Delta\epsilon_y - \nu\Delta\epsilon_z'' - \Delta\epsilon_y'')\frac{E_i''}{1-\nu^2} \quad \ldots\ldots\ldots\ldots\ldots\ldots (14b)$$

in which the conditions of equal strain across the wall is already implied and

$$\Delta\epsilon''_z = (\sigma_{z_o} - \nu\sigma_{y_o})\frac{\phi_i}{E(t_o)};\quad \Delta\epsilon''_y = (\sigma'_{y_o} - \nu\sigma_{z_o})\frac{\phi_i}{E(t_o)}\ (i = 1, \ldots 5) \ldots . \quad (15)$$

are the inelastic (creep) strains produced by prestresses σ_{z_o} and σ_{y_o} caused in concrete by the tendons before long-time losses (2,6). The conditions of equilibrium require

$$\sum_i \Delta\sigma_{z_i} + \frac{A_l E_l}{1-\nu_s^2}(\Delta\epsilon_z + \nu_s\Delta\epsilon_y) + A_{p_z}E_p\Delta\epsilon_z + A_s E_s\Delta\epsilon_s = 0 \ldots \ldots .(16a)$$

$$\sum \Delta\sigma_{y_i} + \frac{A_l E_l}{1-\nu_s^2}(\Delta\epsilon_y + \nu_s\Delta\epsilon_z) + A_{p_y}E_p\Delta\epsilon_z + A_s E_s\Delta\epsilon_s = 0 \ldots \ldots .(16b)$$

in which the subscripts, z and y, refer to vertical and horizontal directions along the wall. The following values were assumed: $A_{p_z} = 0.210$ sq in./in. (0.533 cm^2/cm); $A_{p_y} = 0.394$ sq in./in. (1.00 cm^2/cm); $\sigma_{z_o} = 860$ psi (5.93 N/mm^2); and $\sigma_{y_o} = 1{,}500$ psi (10.3 N/mm^2). The remaining parameters were the same as in the preceding case of shrinkage effect.

Using the values from Eqs. 2 and 5, the solution of Eqs. 14-16 yields the following changes due to creep under prestress from $t_o = 90$ days at $t = 40$ yr (1 psi = 6.89 kN/m^2):

$$\Delta\sigma_{z_i} = 195 \text{ psi}, 83 \text{ psi}, 48 \text{ psi}, 31 \text{ psi}, 16 \text{ psi};\quad \Delta\epsilon_z = -110 \times 10^{-6} \ldots \ldots .(17a)$$

$$\Delta\sigma_{y_i} = 378 \text{ psi}, 169 \text{ psi}, 103 \text{ psi}, 77 \text{ psi}, 46 \text{ psi};\quad \Delta\epsilon_y = -261 \times 10^{-6} \ldots .(17b)$$

In the same manner, the stress changes reached at other times were also analyzed. The results are plotted in Fig. 5.

A similar analysis can be carried out to determine the effect of creep under dead load. The changes obtained in this case are roughly six-times less than those in Eq. 17.

As a by-product of the analysis in both previous cases, one also obtains the prestress losses, $\Delta\sigma_{p_y} = E_p\Delta\epsilon_y$ and $\Delta\sigma_{p_z} = E_p\Delta\epsilon_z$. However, these values as well as the strains in the liner do not differ greatly from the results of the conventional analysis. Thus, the new contribution of the present method of analysis should be seen solely in determining the nonuniformity of stress changes in concrete. The difference with respect to the conventional analysis is essentially given by the difference of the stresses in Fig. 5 from their average value across the wall. According to Fig. 5, the maximum of these differences, in the case of creep effect, is about 150 psi in hoop tension and 100 psi in vertical tension on the exterior face, and 70 psi and 40 psi below the liner.

Overall Stress Redistribution within Structure

As a result of shrinkage, the diameter of the cylindrical shell gradually decreases. However, this is incompatible with the deformation of the foundation slab. This slab is usually unprestressed and because it is sealed on top and buried in the ground it cannot dry and thus exhibits only a small (autogeneous) shrinkage, further diminished by heavy reinforcement and subsoil friction. Consequently,

the time-dependent deformations of the foundation slab may be considered zero, and so additional internal forces will gradually develop near the base of the cylinder. (An effect of this type is well known from the analysis of cylindrical tanks; see p. 38 in Ref. 1, and Refs. 10, 14, and 16.) Furthermore, the foundation slab is relatively very stiff; thus, for the sake of simplicity, the cylindrical shell may be assumed to be rigidly fixed at the base.

Using the age-adjusted modulus method, the well-known solutions for the semi-infinite elastic cylindrical shell (Ref. 8, p. 91) may be applied if elastic modulus E is replaced with E''. Thus

$$\Delta M_z = 2\Delta u D''\beta^2 e^{-\beta z}(\sin\beta z - \cos\beta z) \ldots \ldots .(18a)$$

$$\Delta Q_z = 4\Delta u D''\beta^3 e^{-\beta z}\cos\beta z \ldots \ldots .(18b)$$

$$\text{in which}\quad \beta^4 = \frac{3(1-\nu^2)}{R^2 d^2};\quad D'' = \frac{E'' d^3}{12(1-\nu^2)} \ldots \ldots . \quad (19)$$

Here, z = distance from the base; d = shell thickness [42 in. (1,067 mm)]; R = radius of cylinder [70 ft. (21.3 m)]; $\nu = 0.18$; ΔM_z, ΔQ_z = changes of vertical bending moment and radial shear force; and Δu = radial displacement which would occur at the base from time t_o to time t if the shell were not restrained by the foundation slab.

Shrinkage from $t_o = 10$ days-$t = 40$ yr was estimated to give $\Delta u = 0.17$ in. (4.32 mm). The average E''_i from Eq. 9 is 2.07×10^6 psi (14,270 N/mm^2), which yields $D'' = 13.5 \times 10^9$ lb $\times$ in. (1.525 MN $\cdot$ m). Eq. 18 gives $\Delta M_z = -221$ kips $\times$ in./in. (0.983 MN$\cdot$m/m) at the base of wall ($z = 0$) at $t = 40$ yr.

The bending moment ΔM_z due to shrinkage causes a normal stress change, $\Delta\sigma_z \simeq 750$ psi (5.171 N/mm^2) (tension on the exterior face at the base of the cylinder) and compressive strain $\Delta\epsilon_l = -368 \times 10^{-6}$ in the liner. The decay of these values along the height is rapid and is plotted in Fig. 1(a).

Evaluating ΔQ_z from Eqs. 16, the nominal radial shear stress increment, $\Delta l = Q_z/b$, in which b = depth to reinforcement [$\approx$ 39 in. (991 mm)] is obtained as 75 psi. Note that all of these effects decay rapidly with distance from the base.

The preceding values are based on the assumption that the entire height of the cylindrical wall is exposed. In reality, the bottom part of the wall is buried underground for a certain depth, a; typically $a = 25$ ft (7.6 m). Assuming that the wall is buried to depth a since the time of casting, the free unrestrained shrinkage equals 0 for $z < a$ and Δu is the same as before for $z > a$, with a jump equal to Δu at $z = a$. Approximately, depth a may be considered to sufficiently large for the effect of restraint due to base slab to be negligible near the ground level. Then, using the well-known general solution (Ref. 8, p. 91) to find the solution for boundary conditions $\Delta M_z = 0$ and $u = \Delta u/2$ at $z = a$, one obtains

$$\Delta M_z = \Delta u\, D''\beta^2 e^{-\beta(z-a)}\sin\beta(z-a) \ldots \ldots .(20a)$$

$$\Delta Q_z = \Delta u\, D''\beta^3 e^{-\beta(z-a)}[\cos\beta(z-a) - \sin\beta(z-a)] \ldots \ldots .(20b)$$

Max ΔM_z, which occurs at $z = a \pm \pi/4\beta$, and Max ΔQ_z, which occurs at $z = a$, equal in this case $0.3224\Delta u\, D''\beta^2$, and $0.5\Delta u\, D''\beta^3$, respectively, while in

the previous case of the unburied wall (Eqs. 18), the maximums, both occurring at $z = 0$, equal $2\Delta u\ D''\ \beta^2$ and $4\Delta u\ D''\ \beta^3$. The corresponding normal stress change is $\Delta\sigma_z = 121$ psi (0.834 N/mm^2), the strain is -60×10^{-6}, and the nominal shear stress in concrete is 12 psi (0.0827 N/mm^2). Thus, when the bottom of the wall is buried over a substantial length, the maximum bending moment (as well as normal stresses of concrete and strains of liner) is reduced about six times, and the maximum shear force about eight times [Fig. 1(*b*)].

In reality, however, neither Eqs. 18 nor Eqs. 20 apply. Even in a normal construction schedule, the total height of the wall may remain exposed for a period of several months before the insulation and earthfill are placed, and because of various circumstances that have recently been causing unexpected large delays in construction, a much longer exposure period may actually occur. Due to this drying period, a sizable portion of the final shrinkage for continuously exposed wall may take place under the ground level. Therefore, the actual shrinkage stresses may differ substantially from those for immediate placement of earthfill and eventually might even be closer to those for continuous exposure of the total height of the wall. In any event, the latter case (Eqs. 18) yields an upper bound for the effect of differential shrinkage, while the former case (Eqs. 20) yields the lower bound. A theoretically exact calculation of the effects for a given time schedule is, of course, possible but quite a bit more complicated.

Creep of concrete produced by hoop prestress of the cylindrical shell also causes a relative radial displacement between the shell and the foundation slab. This effect gives rise to bending moments ΔM_{z_1}. However, if the diameter of the shell were kept time-constant along the whole height, a relaxation of the initial elastic secondary bending moments due to prestressing would occur. These changes must be superimposed upon ΔM_{z_1}, and it can be shown that they exactly offset ΔM_{z_1} if the hoop prestress is considered time-constant. (If the long-time prestress loss is considered, the net result would be a small change of bending moment, opposite to ΔM_{z_1}; this small change may be neglected in practice.) It may thus be concluded that creep due to hoop prestress produces no appreciable stress change in addition to elastic secondary moments due to prestressing. This conclusion also follows from a well-known general theorem stating that secondary moments are not altered by creep if the structure is homogeneous in creep properties and no changes in statical system occur. These conditions are met as long as the differences in creep properties between various cross sections along the height are neglected. The stress caused by the long-time increase in the diameter of the shell due to the Poisson effect under vertical prestress and dead weight is also zero, for the same reasons.

Differences in shrinkage with regard to the cylindrical wall also appear in the dome because it dries faster (due to smaller thickness) and has a higher meridional prestress, and in the ring because it dries much slower (due to greater thickness). In contrast to the previous case, creep also produces additional stress redistribution that is due to differences in creep between cross sections drying at different rates. All these effects decay away from the ring and in general are probably less than those near the base. They can be minimized by tendon arrangement that permits omission of the ring.

Furthermore, a somewhat slower drying than that in the cylindrical wall is also encountered in the vertical buttress strips for anchoring hoop tendons. Thus, their vertical creep and shrinkage shortening tends to be less than that

of the cylindrical wall, which produces a shear stress, $\Delta\tau_{yz}$, in the vertical radial section between the buttress and the wall. By similar consideration as before, it has been estimated that $\Delta\tau_{yz} \approx 50$ psi (0.345 N/mm^2) due to differences in creep, and 120 psi (0.828 N/mm^2) due to differences in shrinkage, at $t = 40$ yr. (It is, of course, beneficial to design the shell without hoop tendons and leave out the buttresses.)

More accurate results than these presented herein can be reached with a finite element program. The same program as for the elastic analysis with thermal strains can be used if the age-adjusted effective modulus method is adopted.

Analysis of Results, Stress Relief by Cracking, and More Accurate Methods

The preceding calculations indicated the approximate maximum changes of stresses and strains, shown in Table 1. It is obvious that the tensile stresses are so large that the prestress of the structure cannot prevent cracking. Neverthe-

TABLE 1.—Approximate Concrete Stresses and Liner Strains Caused by Shrinkage and Creep (No Cracking Assumed)

Item (1)	Stress on Exterior Face: Hoop, in pounds per square inch (2)	Stress on Exterior Face: Vertical, in pounds per square inch (3)	Stress below Liner: Hoop, in pounds per square inch (4)	Stress below Liner: Vertical, in pounds per square inch (5)	Nominal shear (6)	Strain of Liner: Hoop $\times 10^{-6}$ (7)	Strain of Liner: Vertical $\times 10^{-6}$ (8)
(*a*) General Cross Section							
Shrinkage	900	900	−200	−200	0	−200	−200
Creep	500	270	−50	−30	0	−260	−110
Total	1,400	1,170	−250	−230	0	−460	−310
(*b*) Additional at Base							
Shrinkage	−135[a] −22[b]	750[a] 120[b]	135	−750[a] −120[b]	75[a] 12[b]	0	−360[a] −60[b]
(*c*) Superimposed Maximums							
Shrinkage	900	1,650[a] 1,020[b]	−200	−950[a] −320[b]	75[a] 12[b]	−200	−560[a] −260[b]
Creep	500	270	−50	−30	0	−260	−110
Total	1,400	1,920[a] 1,290[b]	−250	−980[a] −350[b]	75[a] 12[b]	−460	−670[a] −370[b]

[a] Upper bound.
[b] Lower bound.

Note: These stress values are strictly comparative, i.e., to be compared with stresses due to sustained operating temperature. Actual values, as relieved by cracking, are much less (1 psi = 6.89 kn/m^2).

less, knowledge of these stress values is useful as a means of comparison with stresses produced by other loads in service conditions. In particular, the stress values found are higher than those due to sustained operating temperature, which are of the same nature because they also represent self-equilibrating stress fields and are also relieved by cracking of concrete.

However, it should not be inferred from the foregoing comments that creep and shrinkage are very important effects, because sustained operating temperature itself represents a loading of small significance as compared with other loads, and the overriding criterion for the structure is the limit state of internal pressure. If the stresses due to shrinkage and creep should actually be taken into account in design, it would be necessary to calculate the stress relief due to cracking, which is likely to be quite substantial (and is admissible in the containment shells). The local liner strain near the base will also be reduced by liner slip. The well-known finite element methods of analysis for cracking concrete structures can be combined with the age-adjusted effective modulus method used herein to provide realistic estimates. With regard to the criteria to be imposed on cracking of this type, two types of effects should be distinguished.

One type is the overall straining of the structure by differential creep and shrinkage (e.g., the effects near the base). These can be treated similarly to the effects of operating temperature and can be adequately characterized in terms of a bending moment, an axial force, and a shear force. As one possible approach in design, interaction diagrams for the ultimate values or the permissible values of these forces can be used (11).

The second type is the local straining within a general cross section of wall, in which no curvature change occurs. This effect is of a somewhat different nature, because the stress distributions are not of the type that can be produced by a bending moment. The cracks penetrate to a relatively shallow depth of cross section and, therefore, the cracked concrete is more strongly restrained by the underlying uncracked concrete, causing the cracks to be narrower and more densely distributed. Under such conditions, concrete exhibits considerable ductility in tension, developing a system of microcracks, rather than failing by one large crack. Therefore, this type of cracking due to creep and shrinkage is certainly less damaging (and less important) than the overall straining considered before. It occurs in all types of structures, but it has not yet been analyzed in detail. Routine counter-measures are being taken by placing the so-called shrinkage and temperature reinforcement near the face, which has the purpose of reducing crack width and depth and of preserving the integrity of the concrete. Nevertheless, in a consistent and rational approach, which seems to be worthwhile in the case of reactor containments, one should not ignore these stresses and cracks, especially if other effects of lesser magnitude are being accounted for in design. The finite element solutions that include cracking may be used to determine the average tensile strain of concrete in the cracked zone. On its basis one can determine the size and the spacing of reinforcement that is needed to limit the width of cracks to a certain value and to reduce their depth.

Conclusion

Creep and shrinkage effects in reactor containments are not negligible. They are more important than those of the operating temperature gradient.

Acknowledgments

Grateful appreciation is due to A. K. Gupta for his assistance in formulating the problem. S. L. Chu is to be thanked for supervising the investigation, and B. Erler and A. K. Gupta for their valuable suggestions and review of the manuscript. A small portion of the work of the first author during preliminary considerations as well as some of the final calculations was supported through the National Science Foundation Grant GK-26030 to Northwestern University.

References

1. Bažant, Z. P., *Creep of Concrete in Structual Analysis* (in Czech), State Publishing House of Technical Literature, Prague, Czechoslovakia, 1966, p. 186.
2. Bažant, Z. P., "Prediction of Concrete Creep Effects Using Age-Adjusted Effective Modulus Method," *Journal of the American Concrete Institute*, Vol. 69, 1972, pp. 212-217.
3. Bažant, Z. P., "Creep and Shrinkage Effects in Nuclear Reactor Containment Shells," *Report No. SAD-159*, Sargent and Lundy, Engineers, Chicago, Ill., July, 1974.
4. Bažant, Z. P., "Theory of Creep and Shrinkage in Concrete Structures: A Précis of Recent Developments," *Mechanics Today*, Vol. 2, edited by S. Nemat-Nasser, Pergamon Press, New York, N.Y., 1975, pp. 1-93.
5. Bažant, Z. P., and Najjar, L. J., "Nonlinear Water Diffusion in Nonsaturated Concrete," *Materials and Structures*, Paris, France, Vol. 5, 1972, pp. 3-20.
6. Bažant, Z. P., and Najjar, L. J., "Comparison of Approximate Linear Methods for Concrete Creep," *Journal of the Structural Division*, ASCE, Vol. 99, No. ST9, Proc. Paper 10006, Sept., 1973, pp. 1851-1874.
7. Bažant, Z. P., and Wu, S. T., "Creep and Shrinkage Law of Concrete at Variable Humidity," *Journal of the Engineering Mechanics Division*, ASCE, Vol. 100, No. EM6, Proc. Paper 10995, Dec., 1974, pp. 1183-1209.
8. Billington, D. P., *Thin Shell Concrete Structures*, McGraw-Hill Book Co., Inc., New York, N.Y., 1965, pp. 89-110.
9. Bruegger, J. P., "Methods of Analysis of the Effects of Creep in Concrete Structures," thesis presented to University of Toronto, at Toronto, Canada, in 1974, in partial fulfillment of the requirements for the degree of Master of Applied Science.
10. Ghali, A., and Bazaraa, A. R., "Effect of Shrinkage and Temperature Variation on Cylindrical Concrete Tanks," *Proceedings of the International Association for Shell Structures Symposium*, Warsaw, Poland, Sept. 1963, pp. 572-599.
11. Gurfinkel, G., "Thermal Effects in Walls of Nuclear Containments—Elastic and Inelastic Behavior," *Proceedings of the 1st International Conference on Structural Mechanics in Reactor Technology*, Berlin, West Germany, Vol. 5, Part J, Sept., 1972, pp. 277-297.
12. Hansen, T. C., and Mattock, A. H., "Influence of Size and Shape of Member on the Shrinkage and Creep of Concrete," *Journal of the American Concrete Institu* Vol. 63, 1966, pp. 267-290.
13. L'Hermite, R. G., and Mamillan, M., "Further Results of Shrinkage and Creep Tests," presented at *International Conference on the Structure of Concrete*, held in 1965 at Imperial College, London, England; published by Cement and Concrete Association, London, England, 1968, pp. 423-433.
14. Neville, A. M., and Dilger, W., *Creep of Concrete: Plain, Reinforced, Prestressed*, North Holland Publishing Co., Amsterdam, the Netherlands, 1970.
15. *Standard Code for Concrete Reactor Vessels and Containments*, American Society of Mechanical Engineers Boiler and Pressure Vessel Code, Section III, Div. 2, and *American Concrete Institute Standard 359*, 1974.
16. Stern, U., "Untersuchungen über das Schwind-und Kriechverhalten von Kreiszylinderschalen aus Beton," *Wiss. Zeitschrift der Hochsule für Architektur und Bauwesen*, Weimar, Vol. 13, 1965, pp. 549-556.
17. Tan, C. P., "Concrete Containments for Reactors—State-of-the-Art," *Journal of the*

Structural Division, ASCE, Vol. 96, No. ST7, Proc. Paper 7424, July, 1970, pp. 1543-1566.
18. Reinhardt, P., and Chadha, G., "Temperature Stresses in Prestressed Concrete Walls of Containment Structures," *Prestressed Concrete Institute Journal*, Vol. 19, Jan.-Feb., 1974, pp. 76-85.

Appendix II.—Notation

The following symbols are used in this paper:

A = area of cross section;
D = cylindrical bending stiffness of wall (Eq. 19);
E = Young's modulus;
E'' = age-adjusted effective modulus (Eq. 4);
h, h_e = pore humidity and environmental humidity;
M = bending moment;
Q = shearing force;
t = time = age of concrete in days;
t_o = start of drying exposure or start of creep effect;
β = parameter (Eq. 19);
ϵ_{sh} = unrestrained linear shrinkage;
ϵ, σ = normal strain and stress;
ν = Poisson's ratio;
ϕ = creep coefficient = (creep strain)/(initial elastic strain); and
χ = aging coefficient (Eq. 4).

Subscripts

i = ith layer;
l = steel liner;
p = prestressing steel;
s = nonprestressed steel; and
x, y, z = Cartesian axes (x being normal to the wall, y vertical).

11632 CREEP AND SHRINKAGE IN REACTOR CONTAINMENT

KEY WORDS: **Creep;** Loading; **Nuclear reactor containment;** Reactors; **Shrinkage; Structural engineering; Temperature gradients**

ABSTRACT: The nonuniformity of creep and shrinkage caused by drying, and to a lesser extent by temperature gradients, causes significant self-straining in containment shells. This condition can be of two types: (1) Local, within the cross section of the wall, or (2) global, due to differences in the deformation of the cylindrical shell and foundation slab, or the dome, the ring, and the hoop tendon buttresses. By approximate calculations, in which cracking is neglected, these effects are shown to be quite significant as compared with other loads in service conditions, whose effect is also normally evaluated without consideration of cracking. For quantitative design predictions, the stress relief due to cracking must be considered. By means of a numerical example, it is demonstrated that the age-adjusted effective modulus method permits a very simple analysis of these effects.

REFERENCE: Bazant, Zdenek P., Carreira, Domingo J., and Walser, Adolf, "Creep and Shrinkage in Reactor Containment Shells," *Journal of the Structural Division,* ASCE, Vol. 101, No. ST10, **Proc. Paper 11632**, October, 1975, pp. 2117-2131